

Metadata of the chapter that will be visualized in SpringerLink

Book Title	Chaotic Systems with Multistability and Hidden Attractors	
Series Title		
Chapter Title	Globally Attracting Hidden Attractors	
Copyright Year	2022	
Copyright HolderName	The Author(s), under exclusive license to Springer Nature Switzerland AG	
Corresponding Author	Family Name	Sprott
	Particle	
	Given Name	Julien Clinton
	Prefix	
	Suffix	
	Role	
	Division	
	Organization	University of Wisconsin-Madison
	Address	Madison, WI, USA
	Email	sprott@physics.wisc.edu
Abstract	The many examples in the previous chapters should leave no doubt that hidden attractors are common in nonlinear dynamical systems. Remarkably, hidden attractors can have basins that fill the entire space with every initial condition on the attractor. Two such examples are shown here.	

Globally Attracting Hidden Attractors



Julien Clinton Sprott

1 **Abstract** The many examples in the previous chapters should leave no doubt that
2 hidden attractors are common in nonlinear dynamical systems. Remarkably, hidden
3 attractors can have basins that fill the entire space with every initial condition on the
4 attractor. Two such examples are shown here.

5 1 Introduction

6 The many examples in the previous chapters should leave no doubt that hidden
7 attractors are common in nonlinear dynamical systems. Previous authors have echoed
8 the claim that they are hard to find because there is no systematic method to identify
9 initial conditions in their basin of attraction.

10 Thus it is fitting to temper those claims with some examples of hidden attractors
11 that are *globally* attracting. Not only is every initial condition in their basin of
12 attraction, but every initial condition lies on the attractor, and thus they could hardly
13 be less hidden. Furthermore, such attractors have been known and studied long before
14 the recent hoopla about hidden attractors, and they have other remarkable properties
15 to be recounted here.

16 2 Conservative Nosé–Hoover System

17 The interest in chaotic systems whose orbit visits the entire state space (called
18 *ergodic*) arose long ago from a quest among molecular dynamicists to find a simple

J. C. Sprott (✉)
University of Wisconsin-Madison, Madison, WI, USA
e-mail: sprott@physics.wisc.edu

© The Author(s), under exclusive license to Springer Nature Switzerland AG 2022
X. Wang et al. (eds.), *Chaotic Systems with Multistability and Hidden Attractors*,
Emergence, Complexity and Computation 40,
https://doi.org/10.1007/978-3-030-75821-9_25

595

19 dynamical system that would model the behavior of a harmonic oscillator in thermal
 20 equilibrium with a heat bath at a constant temperature. Prior to the modern chaos
 21 era, it had been assumed that any such model would need many variables. The first
 22 breakthrough came in 1984 when Shuichi Nosé found a Hamiltonian system with
 23 four variables consistent with the necessary condition that the probability distribution
 24 functions of position and momentum should be Gaussian [1] as expected for Gibbs'
 25 canonical ensemble [2].

26 The following year, Bill Hoover showed that Nosé system could be reduced to a
 27 three-dimensional form with the same properties, now known as the Nosé–Hoover
 28 system [3]:

$$29 \quad \begin{cases} \dot{x} = y \\ \dot{y} = -x - zy \\ \dot{z} = y^2 - 1. \end{cases} \quad (1)$$

30 This system was independently discovered in a search for three-dimensional
 31 chaotic flows with five terms and two quadratic nonlinearities, and thus it is also
 32 known as the Sprott A system [4, 5] and has been widely studied. It is the simplest
 33 in a large class of systems with similar properties [6].

34 Absent the zy term, this system is a simple harmonic oscillator with x playing
 35 the role of position, and y is its canonically conjugate momentum. The zy term
 36 represents a nonlinear damping (for positive z) or anti-damping (for negative z) with
 37 z controlled by the \dot{z} equation such that the damping averages to zero when the mean
 38 square momentum $\langle y^2 \rangle$ is unity. Thus z acts as a thermostat, controlling the average
 39 energy of the chaotic oscillator, but allowing it to fluctuate as desired to model an
 40 oscillator in equilibrium with a heat bath [7].

41 System (1) is unusual because it has no equilibrium points, but neither does it
 42 have an attractor because it is derived from a Hamiltonian [8] in which the fourth
 43 variable is a slave of the other three and thus does not influence the dynamics.
 44 Hence the system is conservative with the missing energy in the hidden variable,
 45 and the oscillator is isothermal rather than isoenergetic. Such systems are called
 46 nonuniformly conservative [9], and they share many of the properties of conventional
 47 conservative systems.

48 The third variable allows the system to oscillate chaotically with a chaotic sea
 49 whose Lyapunov exponents are $(0.0139, 0, -0.0139)$ and that stretches to infinity in all
 50 three dimensions, but that encloses an intricate set of nested and intertwined invariant
 51 tori on which the orbits are quasiperiodic with Lyapunov exponents of $(0, 0, 0)$. All
 52 orbits, both in the chaotic sea and on the tori, repeatedly cross the $z = 0$ plane, which
 53 allows the dynamics to be completely characterized by examining a cross section
 54 of the orbit in that plane. In particular, quasiperiodic orbits embedded anywhere in
 55 the chaotic sea will appear as ‘holes’ in that cross section of the flow. The system is
 56 time-reversal invariant under the transformation $(x; y; z; t) \rightarrow (x; -y; -z; -t)$ as
 57 expected for a conservative system.

58 3 Dissipative Nosé–Hoover System

59 There are many ways to add dissipation to a thermostatted oscillator without intro-
 60 ducing equilibrium points and thus producing a hidden attractor. For example, the
 61 constant term in the \dot{z} equation of system (1) can be replaced by a function $f(x)$ that
 62 is everywhere positive:

$$63 \begin{cases} \dot{x} = y \\ \dot{y} = -x - zy \\ \dot{z} = y^2 - f(x). \end{cases} \quad (2)$$

64 Physically, this corresponds to a harmonic oscillator in a heat bath with a one-
 65 dimensional temperature gradient given by $\frac{df}{dx}$.

66 This system with $f(x) = 1 + \varepsilon \tanh(x)$ (corresponding to a temperature that
 67 varies from $1 - \varepsilon$ at $x = -\infty$ to $1 + \varepsilon$ at $x = \infty$ with a maximum gradient of ε
 68 at $x = 0$) was originally proposed and studied by Posch and Hoover in 1997 [10].
 69 For $\varepsilon = 0.38$ it has a hidden chaotic attractor that extends to infinity in all three
 70 dimensions and encloses a region in the vicinity of the origin with conservative tori
 71 and quasiperiodic orbits as shown in Fig. 1 [11]. The chaotic attractor fills the entirety
 72 of its basin of attraction, but with a highly nonuniform measure.

73 The attractor has Lyapunov exponents of (0.0019, 0, -0.0020) and a Kaplan–Yorke
 74 dimension of 2.945. Thus it differs markedly from essentially all the other chaotic
 75 attractors in this book for three-dimensional autonomous flows whose Kaplan–Yorke
 76 dimensions are only slightly greater than 2.0. In fact, the attractor is multifractal with
 77 a capacity dimension of exactly 3.0, and it stretches to infinity in all three dimensions
 78 but with a rapidly decreasing measure. Furthermore, as ε is decreased, the Kaplan–
 79 Yorke dimension further increases until it reaches a value of 3.0 for $\varepsilon = 0$, where the
 80 standard Nosé–Hoover system (1) with a chaotic sea is recovered.

81 As a consequence, its basin of attraction fills the entire space except for a finite
 82 region in the vicinity of the origin wherein tori with quasiperiodic orbits reside. This is
 83 an example of a *Class Ib* basin of attraction [12]. Although it is not a global attractor,
 84 a randomly chosen initial condition not too close to the origin is overwhelmingly
 85 likely to lie in the basin, and it will lie on the attractor, although usually in a region
 86 rarely visited by the orbit.

87 Remarkably, this dissipative system is time-reversal invariant, just like its con-
 88 servative counterpart. The system has a repeller that overlaps the attractor, and that
 89 becomes an attractor when time is reversed. The attractor–repellor pair as shown by
 90 a portion of the orbits in Fig. 2 have only an imperceptible shift in the z -direction of
 91 $\langle z \rangle \approx \pm 1.2 \times 10^{-4}$ with $\langle x \rangle \approx -0.6855$ and $\langle y \rangle = 0$.

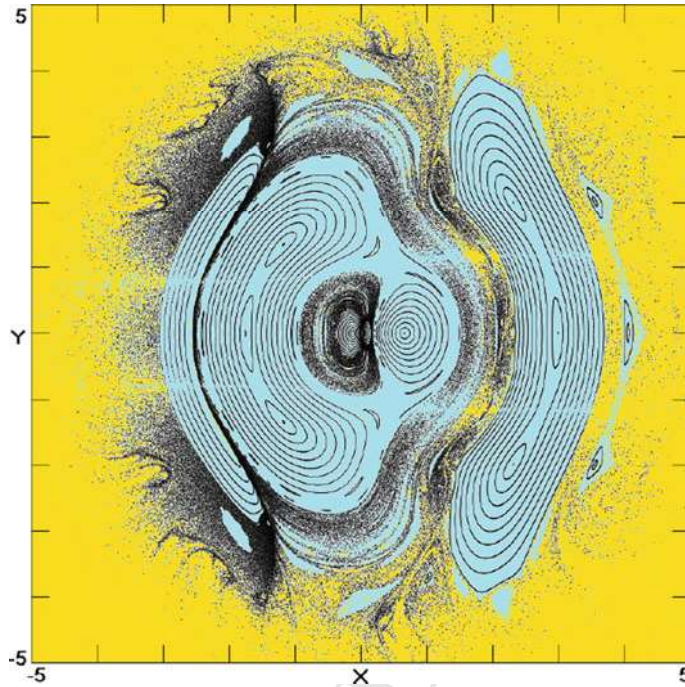


Fig. 1 Cross-section of the orbits in the $z = 0$ plane for system (2) with $f(x) = 1 + 0.38 \tanh(x)$. Blue indicates the regions with conservative tori and quasiperiodic orbits, and yellow indicates the infinite basin of attraction of the dissipative hidden chaotic attractor shown in black [11]

92 4 Buncha System

93 As if the previous case were not remarkable enough, there are variants of the Nosé–
 94 Hoover system that are dissipative and ergodic with a hidden attractor that is the
 95 entirety of the three-dimensional state space. Probably the simplest and most elegant
 96 example is a reduced form of a general class of system proposed and studied by
 97 Buncha Munmuangsaen and collaborators [13] and given by

$$98 \begin{cases} \dot{x} = y \\ \dot{y} = -x - azy \\ \dot{z} = |y| - 1. \end{cases} \quad (3)$$

99 Like the Nosé–Hoover case, this system has a single bifurcation parameter a that
 100 can be put in any of the five terms, and that completely characterizes the system
 101 through a one-dimensional bifurcation diagram as shown in Fig. 3. For $a = 0$ the
 102 system is a simple conservative harmonic oscillator with an amplitude that depends
 103 only on the initial conditions.

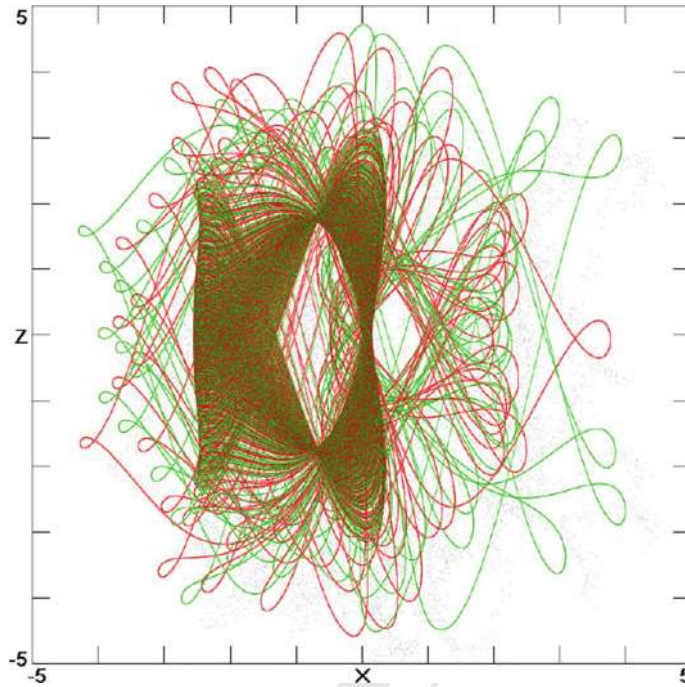


Fig. 2 An orbit on the hidden attractor (in red) and on the corresponding repellor (in green) for system (2) with $f(x) = 1 + 0.38 \tanh(x)$

104 For $a > 0$, there are three distinct regions with bifurcations in the vicinity of
 105 $a = 0.9$ and $a = 2.1$. For a less than about 0.9, the dynamic is dominated by nested
 106 invariant tori with conservative quasiperiodic orbits but surrounded by a dissipative
 107 region with limit cycles and/or strange attractors. In the range of a between about
 108 0.9 and 2.1, there is a conservative region containing nested tori that are linked by
 109 a symmetric pair of dissipative limit cycles and a long-duration chaotic transient
 110 whose orbit eventually collapses onto one of the limit cycles with a riddled basin of
 111 attraction. At $a \approx 2.0$, the limit cycles merge into one large limit cycle at $a \approx 2.07$
 112 that gives birth to a strange attractor surrounding the tori. As a is increased further,
 113 the tori shrink and eventually vanish at $a \approx 3.07$, leaving only dissipative regions
 114 with a single strange attractor that fills all of space.

115 The Kaplan–Yorke dimension of the attractor continues to increase with increasing
 116 a , reaching a maximum of about 2.9924 at $a = 7$ before slowly decreasing, except
 117 for narrow periodic windows in the vicinity of $a = 2.28, 3.78, 4.00$, and 6.00, as well
 118 as other values that are unresolved in Fig. 3. In these periodic windows, there is a
 119 long-duration chaotic transient.

120 Although system (3) exhibits a variety of unusual behaviors, our interest here is in
 121 the regime where there is a single ergodic strange attractor that fills all of space and
 122 thus is technically “hidden” because the system has no equilibrium points. For that

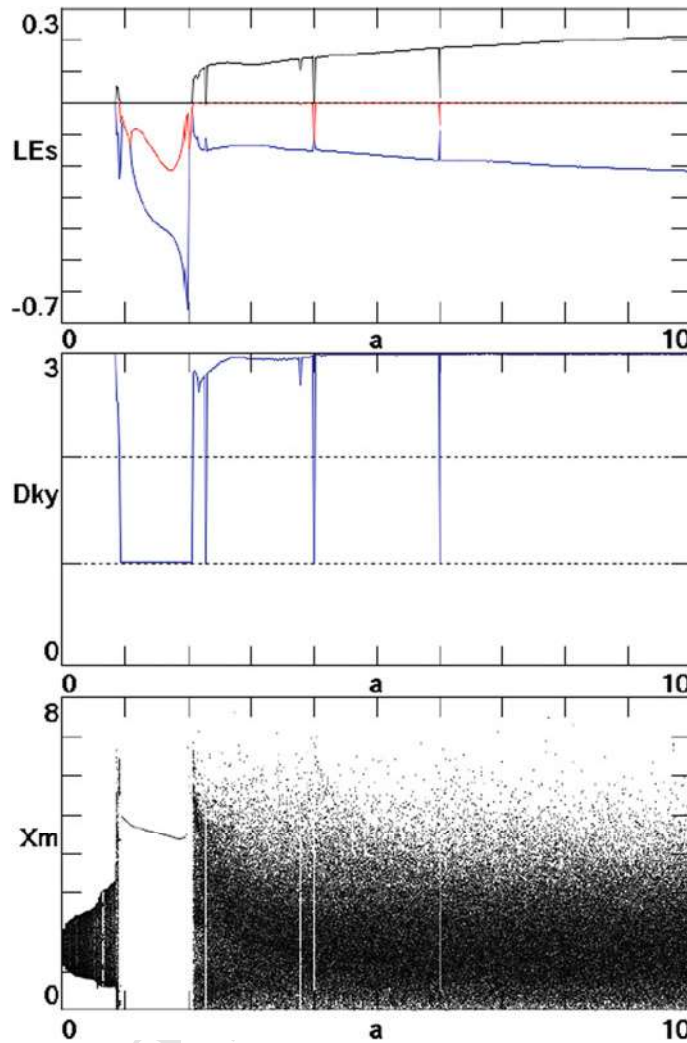


Fig. 3 Lyapunov exponents (LEs), Kaplan–Yorke dimension (Dky), and the local maxima of x (X_m) as a function of the bifurcation parameter a in (3) over the range $0 < a < 10$

123 purpose, we focus on the case $a = 5$ for which the Lyapunov exponents are $(0.1610, 0,$
 124 $-0.1633)$, the Kaplan–Yorke dimension is 2.9858, and the orbit is as shown in Fig. 4.
 125 In this plot, the colors indicate the value of the local largest Lyapunov exponent with
 126 red positive and blue negative. While the attractor appears to be bounded, it has a
 127 fuzzy edge, and after a sufficiently long time the orbit will come arbitrarily close to
 128 every point in the three-dimensional state space.

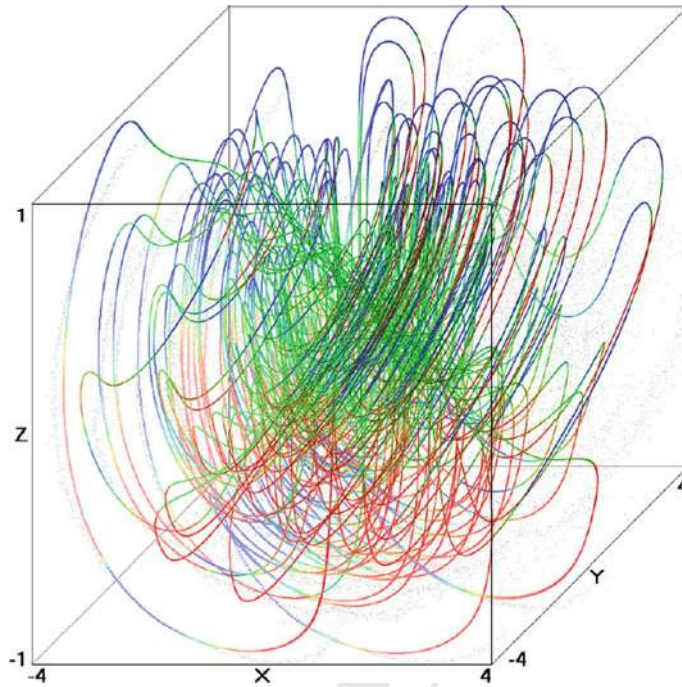


Fig. 4 An orbit on the ergodic strange attractor for system (3) with $a = 5$. The colors indicate the value of the local largest Lyapunov exponent with red positive and blue negative

129 To confirm that the system is ergodic with no embedded tori and quasiperiodic
 130 orbits, it suffices to examine a cross section of the flow at $z = 0$. Figure 5 shows such
 131 a plot. Other than the nullclines at $y = \pm 1$, where the orbit is tangent to the plane,
 132 there are no holes that would indicate a lack of ergodicity. A single orbit eventually
 133 visits every point in the plane, and every initial condition produces the same plot.
 134 Said differently, the attractor is globally attracting with a *Class 1a* basin of attraction
 135 [12], and the attractor fills the whole of its basin.

136 The local largest Lyapunov exponent has a complicated structure as evidenced
 137 by the variations in color. Furthermore, the equations are time-reversible under the
 138 transformation $(x, y, z, t) \rightarrow (x, -y, -z, -t)$ just like the previous cases. When
 139 time is reversed, the attractor becomes a repellor that looks identical to the attractor.
 140 Thus there exists a symmetric strange attractor-repellor pair that is coincident, except
 141 for a tiny offset in the z direction of $\langle z \rangle = \pm 0.0023$, and they exchange roles when
 142 time is reversed.

143 The attractor and repellor are both multifractal with a capacity dimension of
 144 exactly 3.0 but with a highly nonuniform measure that is far from the Gaussian that
 145 characterizes the usual conservative ergodic harmonic oscillator. The probability
 146 distribution functions for the three variables, along with the first six even moments
 147 of the distribution, are shown in Fig. 6. None of the distributions have a sharp cutoff,

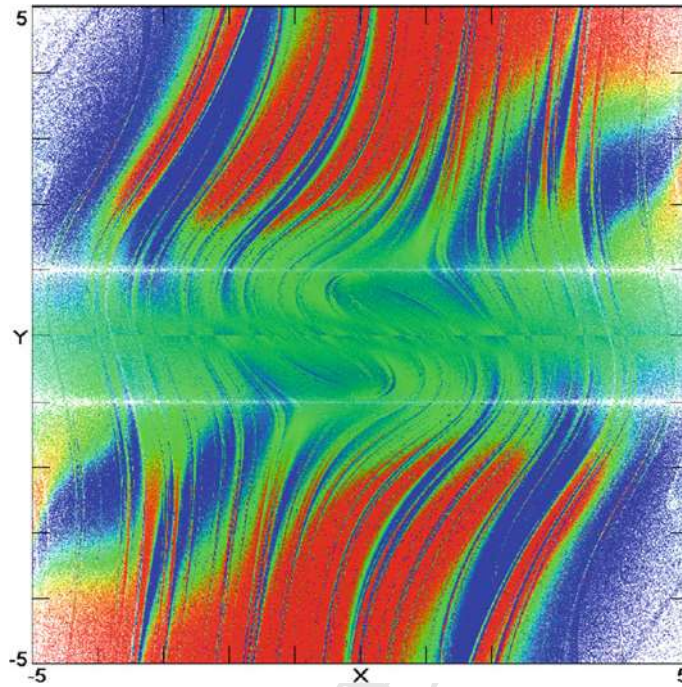


Fig. 5 Cross section of the ergodic strange attractor in the $z = 0$ plane for system (3) with $a = 5$. The colors indicate the value of the local largest Lyapunov exponent with red positive and blue negative

148 but rather they have long tails that extend to infinity in all directions. Hence the
149 attractor and its basin fill the whole of the state space.

150 5 Signum Thermostat Dissipative System

151 Finally, we consider a dissipative chaotic system that is fully ergodic with a measure
152 that more nearly approximates a Gaussian with a hidden global attractor and that is
153 presented here for the first time. This system is a variant of the dissipative Nosé–
154 Hoover system (2) but with the zy term replaced by $2\text{sgn}(z)y$ and is called the signum
155 thermostat [14]. To preserve symmetry in the x probability distribution, $f(x)$ is taken
156 as $f(x) = \exp(-\varepsilon x^2)$ to give

$$157 \begin{cases} \dot{x} = y \\ \dot{y} = -x - 2\text{sgn}(z)y \\ \dot{z} = y^2 - \exp(-\varepsilon x^2). \end{cases} \quad (4)$$

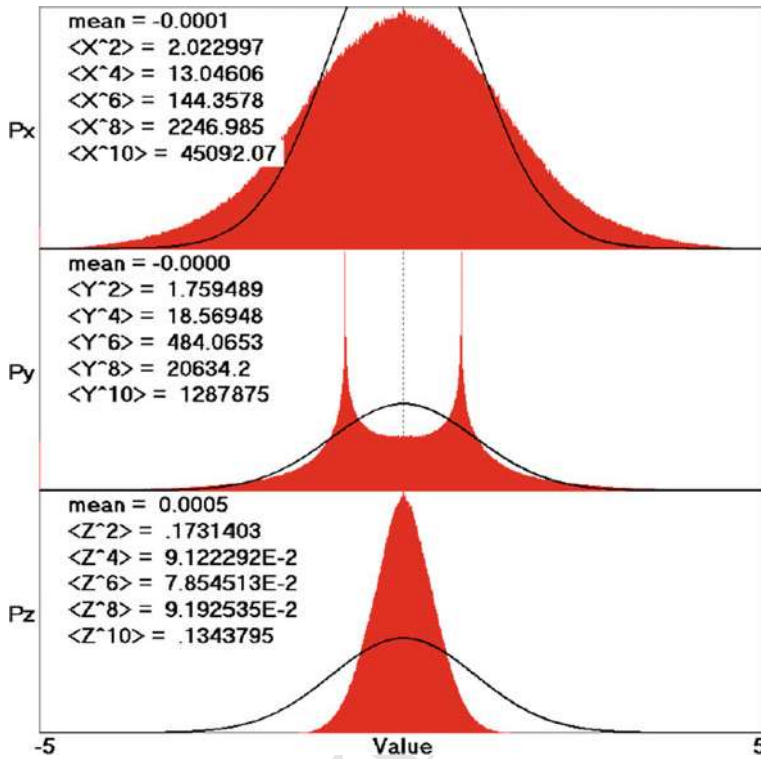


Fig. 6 Probability distribution functions of the ergodic strange attractor for system (3) with $a = 5$. The black curves show a Gaussian distribution with a variance (second moment) of 1.0

Editor Proof

158 Physically, this corresponds to a harmonic oscillator in a heat bath with its highest
 159 temperature at $x = 0$ and that approaches absolute zero at $x = \pm\infty$. Since $f(x) > 0$
 160 for all x , there is no equilibrium point, and so any attractor for the system is hidden
 161 by definition.

162 For $\varepsilon = 0$ (constant temperature), $\exp(-\varepsilon x^2) = 1$, and the system is nonuni-
 163 formly conservative and ergodic with a chaotic sea whose probability distribution is
 164 given exactly by $P(x, y, z) = \exp(-x^2/2 - y^2/2 - 2|z|)/2\pi$. For ε small and posi-
 165 tive, the system is dissipative and ergodic with a strange attractor whose probability
 166 distribution departs only slightly from the case with $\varepsilon = 0$.

167 For example, $\varepsilon = 0.1$ gives the cross section plot at $z = 0$ shown in Fig. 7. Aside
 168 from the nullclines at $y = \pm \exp(-x^2/20)$, there is no indication of quasiperiodic
 169 holes in the plot. The colors show that the local largest Lyapunov exponent has a
 170 considerable structure as is typical of these systems.

171 The evidence that the system is dissipative with a chaotic attractor comes from
 172 the Lyapunov exponents whose values are $(0.03544, 0, -0.3636)$, the Kaplan–Yorke
 173 dimension whose value is 2.9746, and the time-averaged dissipation of $\langle 2\text{sgn}(z) \rangle \approx$
 174 9.2×10^{-3} . The attractor is multifractal with a capacity dimension of 3.0.

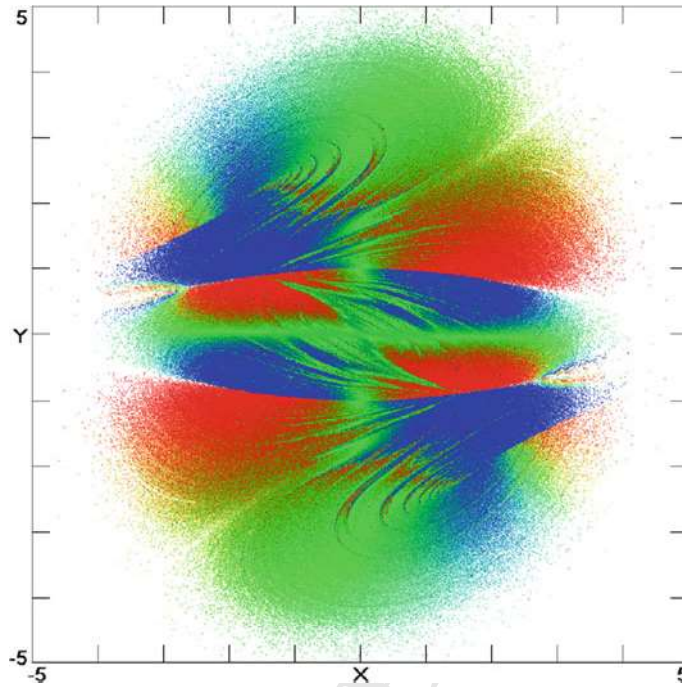


Fig. 7 Cross section of the ergodic strange attractor in the $z = 0$ plane for system (4) with $\varepsilon = 0.1$. The colors indicate the value of the local largest Lyapunov exponent with red positive and blue negative

175 Like the previous systems, this case is time-reversal invariant under the trans-
 176 formation $(x, y, z, t) \rightarrow (x, -y, -z, -t)$ with an attractor-repeller pair that fully
 177 overlap with only a tiny offset in the z -direction. The attractor has a global *Class 1a*
 178 basin of attraction [12], and the attractor fills the entire basin.

179 Figure 8 shows the small departure of the probability distribution functions from
 180 the ones with $\varepsilon = 0$. The dissipative oscillator spends slightly less time in the vicinity
 181 of the origin where it is heated strongly as well as far from the origin where it is
 182 cooled, and relatively more time at intermediate values. Although the tails of the
 183 distributions are suppressed, they still extend to infinity in all directions so that every
 184 initial condition is on the attractor.

185 Smaller values of ε give distributions even closer to a Gaussian and Kaplan-
 186 Yorke dimensions that approach ever closer to the limit of 3.0. The system remains
 187 ergodic for ε up to about 3.4 except for periodic windows with long duration chaotic
 188 transients, whereupon the chaotic attractor is replaced by a globally attracting hidden
 189 limit cycle. This is not surprising since the temperature is an amplitude parameter
 190 that does not affect the dynamic in the conservative constant-temperature case with
 191 a signum thermostat. However, the probability distributions become increasingly
 192 peaked at intermediate values of x and y as ε increases.

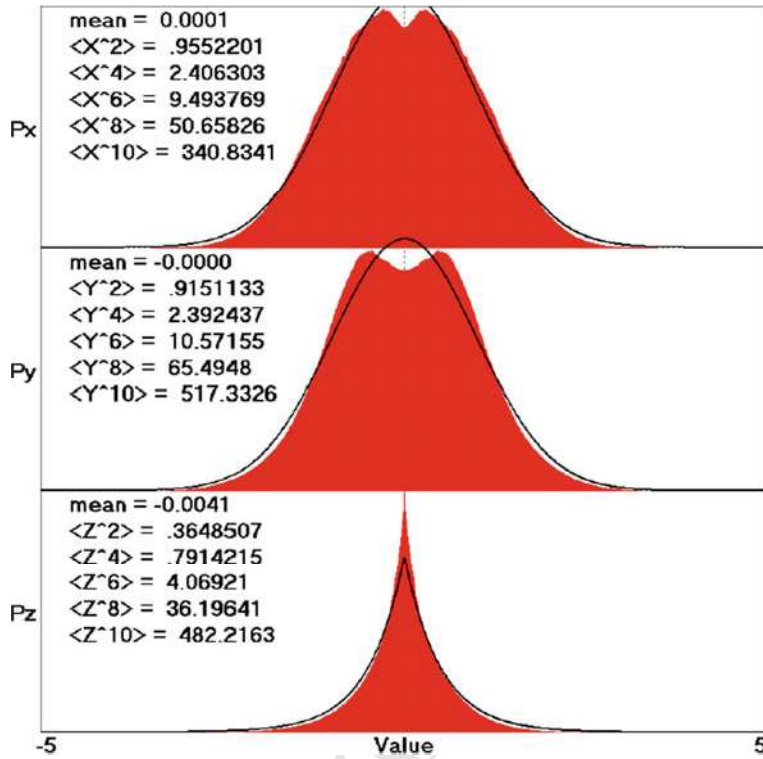


Fig. 8 Probability distribution functions of the ergodic strange attractor for system (4) with $\varepsilon = 0.1$. The black curves show the distributions for $\varepsilon = 0$

Editor Proof

6 Summary and Conclusions

The Nosé–Hoover system is almost certainly the simplest example of a nonuniformly conservative chaotic flow without equilibria, but the chaotic sea coexists with regions of quasiperiodicity. It is the simplest example of a wide class of thermostatted oscillators, which are time-reversal invariant in accordance with Newton’s laws and that exhibit aspects of thermodynamics and statistical mechanics such as a Gaussian probability distribution function. It is possible to eliminate the quasiperiodic regions and obtain systems that are fully ergodic with the orbit visiting every point in space as desired for a realistic physical model.

There are various ways to add dissipation to such systems and produce strange attractors that are hidden and that fill almost the entire state space, typically with a finite region that is occupied by tori with conservative quasiperiodic orbits. Most remarkably, it is also possible to modify the dissipative systems in such a way as to make them fully ergodic with a multifractal strange attractor that is globally attracting and fills the whole of space and yet satisfies the definition of being hidden. Two such

208 examples were given here. These systems may be more realistic models of physical
 209 phenomena than are the purely mathematical models with hidden attractors that
 210 constitute most of the other examples in this book.

211 References

- 212 1. S. Nosé, A unified formulation of the constant temperature molecular dynamics methods. J.
 213 Chem. Phys. **81**, 511–519 (1984)
- 214 2. J.W. Gibbs, *Elementary Principles in Statistical Mechanics* (Charles Scribner's Sons, New
 215 York, 1902)
- 216 3. W.G. Hoover, Canonical dynamics: equilibrium phase-space distributions. Phys. Rev. A **31**,
 217 1695–1697 (1985)
- 218 4. J.C. Sprott, Some simple chaotic flows. Phys. Rev. E **50**, R647–R650 (1994)
- 219 5. W.G. Hoover, Remark on 'some simple chaotic flows'. Phys. Rev. E **51**, 759–760 (1995)
- 220 6. W.G. Hoover, C.G. Hoover, *Simulation and Control of Chaotic Nonequilibrium Systems* (World
 221 Scientific, Singapore, 2015)
- 222 7. J.C. Sprott, W.G. Hoover, Harmonic oscillators with nonlinear damping. Int. J. Bifurc. Chaos
 223 **27**, 1730037 (2017)
- 224 8. C.P. Dettmann, G.P. Morriss, Hamiltonian reformulation and pairing of Lyapunov exponents
 225 for Nosé-Hoover dynamics. Phys. Rev. E **55**, 3693–3696 (1997)
- 226 9. J. Heidel, F. Zhang, Nonchaotic behavior in three-dimensional quadratic systems Π : the con-
 227 servative case. Nonlinearity **12**, 617–633 (1999)
- 228 10. H.A. Posch, W.G. Hoover, Time-reversible dissipative attractors in three and four phase-space
 229 dimensions. Phys. Rev. E **55**, 6803–6810 (1997)
- 230 11. J.C. Sprott, W.G. Hoover, C.G. Hoover, Heat conduction, and the lack thereof, in time-reversible
 231 dynamical systems: generalized Nosé-Hoover oscillators with a temperature gradient. Phys.
 232 Rev. E **89**, 042914 (2014)
- 233 12. J.C. Sprott, A. Xiong, Classifying and quantifying basins of attraction. Chaos **25**, 083101
 234 (2015)
- 235 13. B. Munmuangsaen, J.C. Sprott, W.J. Thio, A. Buscarino, L. Fortuna, A simple chaotic flow
 236 with a continuously adjustable attractor dimension. Int. J. Bifurc. Chaos **25**, 1530036 (2015)
- 237 14. J.C. Sprott, Ergodicity of one-dimensional oscillators with a signum thermostat. Comput. Meth-
 238 ods Sci. Technol. **24**, 169–176 (2018)